# SPECTRAL CHARACTERIZATIONS OF CENTRIFUGAL FAN NOISE VIA URANS-BASED NOISE PREDICTION METHOD

Ali ZAMIRI[1], Hyeon Joon OH[2], Young J. MOON[1]

[1] *Computational Fluid Dynamics and Acoustics Laboratory, School of Mechanical Engineering, Korea University, Seoul, 136-701, Rep. of Korea*

[2] *Samsung Electronics Co., Ltd, Suwon, Rep. of Korea*

## SUMMARY

Noise prediction of centrifugal fan is difficult because flows are turbulent and locally separated in the blade flow passages. It is important to realize that the far-field acoustics are dominated by the internal pressure fluctuations inside the fan motor housing, comprised of rotating impellers, diffusers, return channels, motor stands, etc. In the present study, an uRANS-based approach with k-ω SST turbulence model is used to predict the fan performance as well as the noise characteristics of the centrifugal fans. The near-field pressure fluctuation spectra computed by uRANS are in good agreement with the measured far-field SPL spectra in a relative manner, if the flow rate is not too off from the peak efficiency. It is expected that the uRANS can be used as a tool for optimizing the fan noise characteristics, as long as the fan is enclosed with the fan motor housing.

## INTRODUCTION

Centrifugal fans play an important role in a wide range of industrial applications due to high pressure rise and large capacity of mass flow rate, compared to their sizes. Furthermore, it has been reported that the centrifugal fans can significantly improve the productivity and safety in air ventilation systems and electronics industries. On the other hand, the moderate efficiency and the high noise level still remain as an issue.

The noise generated by the centrifugal fan is generally broadband and tonal. The broadband noise is usually generated by flow separations and turbulent flows, acting on the solid surfaces of the impeller and fan casing [1], [2]. The tonal noise is, however, produced by strong interactions between the impeller and diffuser blades. The tonal noise corresponds to the blade passing

frequency (BPF) and its higher harmonics, varying with the rotational speed and impeller blade counts [3].

Many experimental studies have been conducted for better understanding of the flow structures and noise generation mechanisms inside the centrifugal fans [4], [5]. Neise presented an extensive review on noise reduction of the centrifugal fan [6], [7]. With the development of numerical methods and high performance computers, computational methods have widely been used to predict the fan noise [8].

Numerical simulation of turbomachinery is still a difficult task since flows are turbulent and often separated in the blade passages. It has been shown that the unsteady Reynolds averaged Navier-Stokes (uRANS) can be used for aerodynamic analysis of the centrifugal fans but still questionable for aeroacoustic prediction, for which LES (large eddy simulation) is generally considered as a more reliable tool. Besides, most of the numerical studies have been focused on isolated centrifugal fans impellers, without considering the whole components of centrifugal fan. Thereby studies are mostly concerned with tonal noise via impeller-diffuser interactions [9].

In the case of centrifugal fan with whole geometry, it is conjectured that the baseline curve of the broadband noise spectrum is attributed not only by turbulent fluctuations but also by unsteady pressure fluctuations inside the fan motor. In the present study, a prediction method based on uRANS is used to predict not only the fan performance but also the noise characteristics of the full-scale centrifugal fans, primarily comprised of impellers, diffusers, return channels, and AC electric motor. The present approach will be validated by the experimental measurements, with respect to vacuum pressure/air flow performance curve as well as to the far-field acoustic measurements of the centrifugal fan.

## EXPERIMENTAL SETUP

The experimental measurement was conducted with a full geometry of centrifugal fan (used in vacuum cleaner) for different air flow rates and different impeller blade counts (7, 9 and 13 blades). The fan impeller with diffuser and return channel used in this work is shown in Fig.1-a.

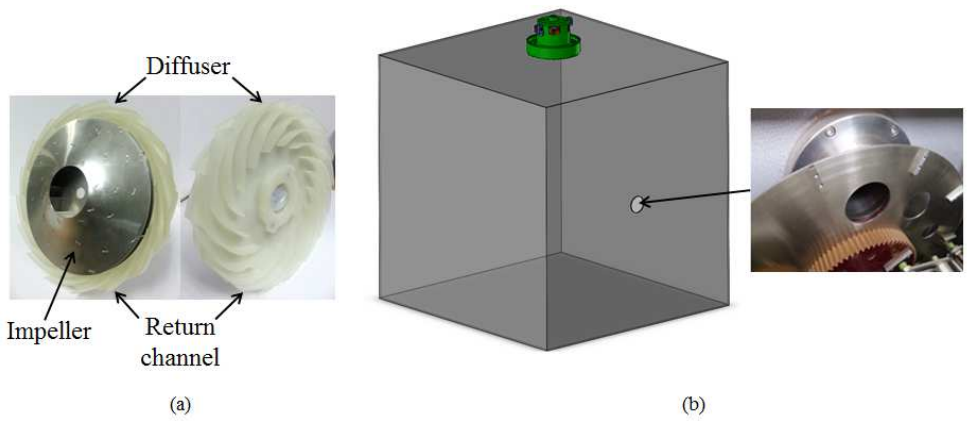


*Figure 1: (a) centrifugal fan impeller-diffuser (upstream and downstream view), (b) schematic of aerodynamic experimental configuration*

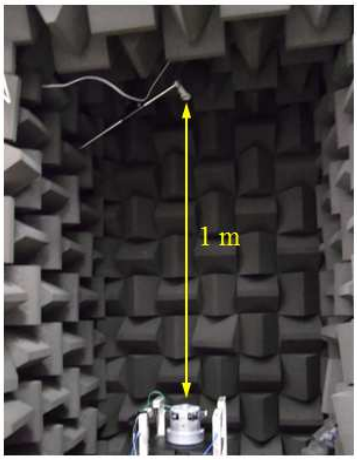


*Figure 2: experimental setup for acoustic measurement*

The aerodynamic measurements were carried out on a test bench equipped with a cubic chamber (0.5 x 0.5 x 0.5 m³), which was placed upstream of the centrifugal fan impeller (Fig.1-b) and a disk-type orifice was designed with adjustable diameters to control the inlet air flow rate (Fig.1-b). Fig.2 illustrates the configuration of acoustic pressure measurements at the far-field in an anechoic chamber. The overall A-weighted sound pressure level emitted by the centrifugal fan was measured at 1.0 meter far from the impeller in a vertical direction. The sound pressure level was measured with 1-5 Hz intervals and the range of measured frequencies was between 0 and 16 kHz.

## COMPUTATIONAL MODELING

### Geometry and grid

Numerical simulations of the unsteady flow in the centrifugal fans were carried out in parallel with the measurements. The complete 3D computational fluid domain for numerical simulation is depicted in Fig.3-a, in which a big chamber is placed upstream of the impeller with the installed orifice. Diffuser, return channel and AC electric motor follow the impeller, and all of the AC motor components are modeled with some simplifications necessary in the numerical simulations to have the almost exact comparison with the experiments (see Fig.3-a). Moreover, for numerical stability and proper physical boundary condition implementation, two fluid volumes are adopted to the computational domain to include proper the inlet and outlet effects. Figure 3-b illustrates the impeller, diffuser and return channel used in the numerical modeling. The total grid for the computational domain is about 11,650,000 cells, consisting of tetrahedral and prism elements (69,1500 prism elements near the wall surfaces), in which the impeller contains 25% of the total meshes.

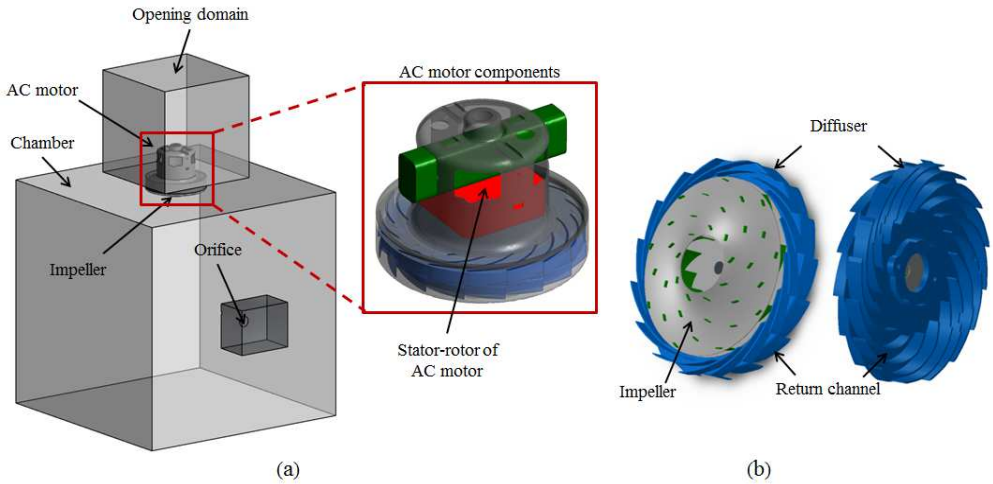


*Figure 3: (a) total view of computational domain, (b) centrifugal fan impeller-diffuser (upstream and downstream view)*

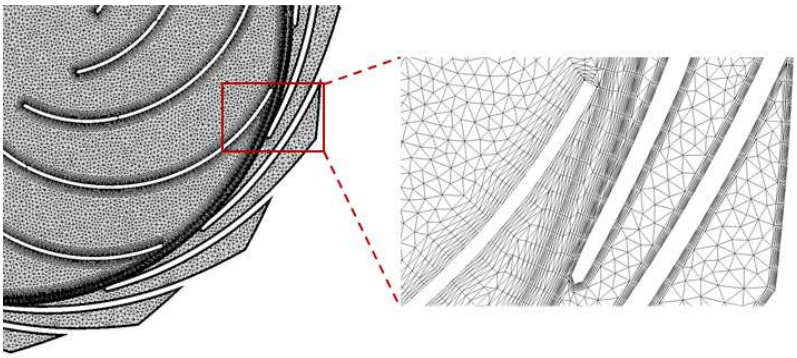

*Figure 4: numerical grid: cross-section plane across the impeller and diffuser*

Figure 4 shows the unstructured mesh on the cross-section plane of the impeller and diffuser (finer meshes used at the impeller-diffuser interface).

## Governing equations

The computation was conducted by solving the three-dimensional, incompressible uRANS equations,

$$\frac{\partial \overline{U_j}}{\partial x_j} = 0 \tag{1}$$

$$\frac{\partial \overline{U_i}}{\partial t} + \overline{U}_j \frac{\partial \overline{U_i}}{\partial x_j} = -\frac{1}{\rho}\frac{\partial \overline{P}}{\partial x_i} + \nu \frac{\partial^2 \overline{U_i}}{\partial x_j \partial x_j} - \frac{\partial}{\partial x_j}\left\{\overline{u_i u_j}\right\} \tag{2}$$

where $\overline{U_i}$ $P$, and $u_i u_j$ is the velocity, pressure, and Reynolds stress tensor. The numerical model used a coupled implicit, pressure based solution technique. Due to low pressure rise, the incompressible flow (air at 25 C) through the rotating impeller was solved in a moving reference frame with a constant impeller rotational speed. The walls of the model were stationary with respect to the reference frame and a no-slip boundary condition was applied. An opening boundary condition with ambient pressure (101,325 kPa) was set to the inlet and outlet boundaries to allow the vortices to pass the boundary in and out at the same time. For the turbulence closure model, a

$k-\omega$ shear stress transport model (SST) was used, which is known as the most accurate and efficient model for aerodynamic simulations [10].

For steady simulations, a frozen rotor was chosen at the interface of impeller-diffuser, which the frame of reference is changed but the relative orientation of the components across the interface is fixed. In the case of transient simulations, the second order backward Euler scheme was applied for the time discretization and the transient rotor-stator was used for the impeller-diffuser interface. Considering the impeller grid rotation corresponding to the rotational speed, a time step of 5-degree incremental angle was used. The transient simulation was carried out until the fluctuations of the flow field become time periodic, as judged by the pressure fluctuations at the impeller-diffuser interface.

## AERODYNAMIC & AEROACOUSTIC ANALYSES

Due to large scale disparity in aeroacoustics, a hybrid approach (CFD/CAA) is often chosen for the computational investigation of the centrifugal fan noise. For the hybrid method, transient Navier-Stokes equations are solved to calculate the unsteady velocity and pressure and then these results are used as an acoustic source for the wave equation to obtain the far-field acoustics.

As far as characterization of the fan noise is concerned, it is important to realize that the far-field acoustics are very much dominated by the internal pressure fluctuations inside the fan housing. In this study, the near-field pressure fluctuations are computed by uRANS, modeling all of the centrifugal fan motor components such as impeller, diffuser, return channel, and AC motor, etc., though some simplification was not unavoidable. The numerical results are compared with measurements in two different aspects: 1) aerodynamic performance analysis and 2) aeroacoustic analysis.

### Aerodynamic performance analysis

Four cases of different orifice diameters (16, 19, 23 and 50 mm) were computed by steady uRANS method for the 7-blade impeller to validate with the experiment the effect of inlet air flow rate on the aerodynamic performance. The velocity magnitude and pressure contours on a plane cut through the center of the impeller and diffuser are compared in Fig.5 for different flow rates.

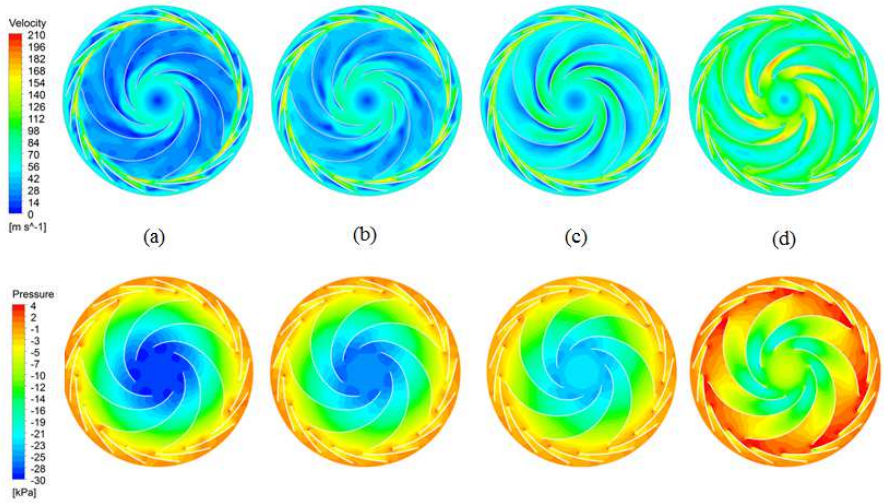


*Figure 5: velocity and pressure contours at the impeller-diffuser cross-section plane for four orifice diameters: (a) 16, (b) 19, (c) 23, (d) 50 mm*

*Table 1: comparison of vacuum pressure and flow rate for experiment and computation for different orifices*

| Orifice diameter (mm) | Vacuum pressure (kPa) | | Flow rate (l/sec) | |
|---|---|---|---|---|
| | Experiment | Computation | Experiment | Computation |
| 16 | 27.39 | 27.90 | 23.93 | 23.80 |
| 19 | 22.45 | 21.24 | 30.93 | 31.21 |
| 23 | 15.35 | 15.75 | 38.18 | 37.99 |
| 50 | 1.14 | 1.60 | 50.99 | 51.25 |

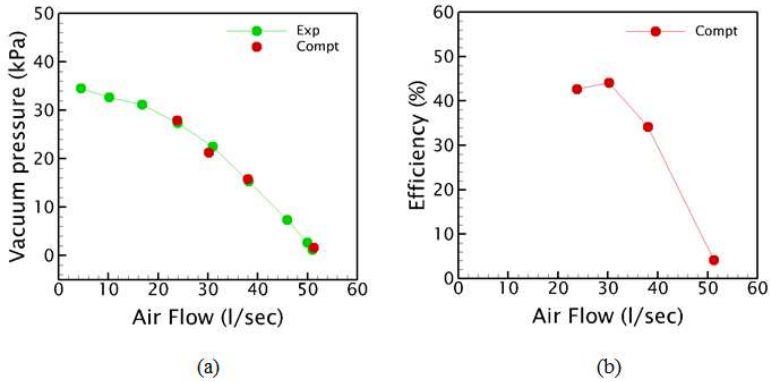


*Figure 6: (a) comparison of vacuum pressure vs. air flow rate performance curve, (b) efficiency curve (numerical)*

In Fig.6-a, the vacuum pressure versus air flow rate is compared between computation and experiment. Once the flow rate is increased beyond 30 (l/sec), the vacuum pressure decreases rapidly due to energy loss in the blade flow passages (see Fig.6-b). Fig.6-b illustrates the numerical efficiency curve of the centrifugal fan, in which the mechanical loss of the motor is not taken into account. Table 1 summarizes the vacuum pressure and flow rate of experimental measurements for four different orifices compared with numerical simulations. The comparison of results shows that the numerical results are in good agreement with the experiments in aspect of aerodynamic analysis.

## Near-field spectral characteristics for different flow rates

In order to obtain the near-field spectrum, a pressure was monitored at the mid-point between two diffuser blades along the impeller-diffuser interface (location of the monitoring point is depicted in Fig.7-a). The time evolution of the pressure versus the normalized time is presented in Fig.7-b, where the time periodic pressure signal also indicates the convergence of the unsteady solution.

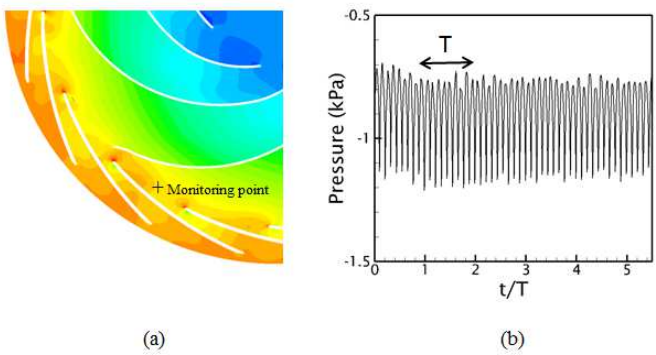


*Figure 7: (a) monitoring point, (b) pressure fluctuation at monitoring point versus normalized time; T is a period for one revolution of the impeller*

The near-field pressure fluctuation spectra predicted by the present uRANS approach are compared in Fig. 8 to the far-field sound pressure level spectra measured in experiment for four different orifice diameters (7-blade impeller). Note first that the absolute SPL ranges are different for computation and experiment, but the total difference of SPL between minimum and maximum is the same as 120 dB. Secondly, the SPL range of the orifice diameter of 16 mm and 7-blade impeller is used as a reference for all cases so that comparisons can be made in a relative sense between experiment and computation and among the cases as well. This relative comparison has been tested for impellers with different blade counts and even for different fan, e.g. cross-flow fan used for an air-conditioner indoor unit [11].

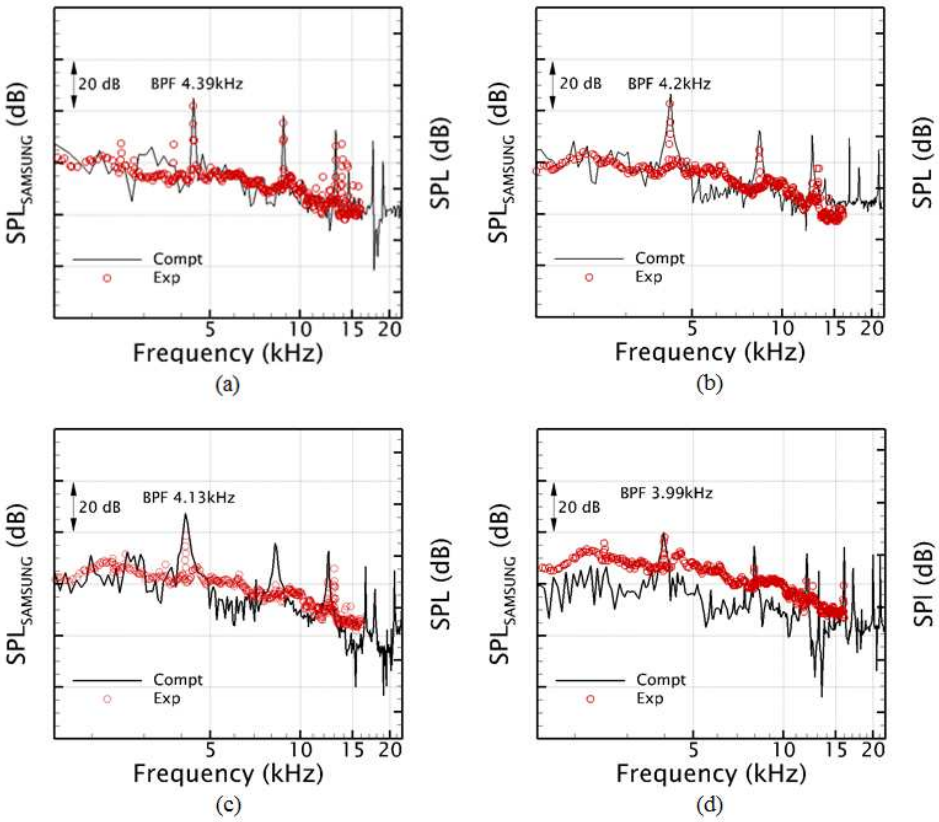


*Figure 8: comparison of numerical near-field sound pressure level spectrum with far-field experiment spectrum for orifice diameter (7-blade impeller): (a) 16 mm, (b) 19 mm, (c) 23 mm, (d) 50 mm*

As shown in Fig. 8, the present numerical modeling with a $k-\omega$ shear stress transport model (SST) represents reasonably well the spectral characteristics of the internal pressure fluctuations inside the fan motor housing. It was found that the comparison is surprisingly good not only for the tonal peaks (BPF and harmonics) but also the broadband part of the spectrum. First, it may be conjectured that the baseline curve of the spectrum is mostly attributed by the unsteadiness originated inside the fan housing, mostly attributed to the interactions of rotating blades with diffusers, return channel, motor stands, etc. Secondly, those interactions can be sufficiently prevalent to be captured by the present numerical modeling with uRANS.

It is, however, interesting to note that as the flow rate increases from 16 to 50 mm, the computation under-predicts the baseline of the spectrum. As observed in the experiment, the tonal peaks are considerably masked by the increased broadband part. In this case, the uRANS approach cannot predict well the unsteadiness caused by turbulent fluctuations. On the other hand, note also that 50 mm case is quite off from the peak efficiency and should not be a major concern, as far as the characterization of the fan noise is concerned.

### Sensitivity of uRANS on the numeric

A numerical test was conducted with using a different turbulence model and a different unstructured grid to validate the noise prediction via uRANS with the experiment. In the case of $k-\varepsilon$ model with the same grid resolution ($11.65\times10^6$ mesh elements), there is a spurious peak around 2 kHz in the spectrum, which is not present in the experiment (see the orange circle in Fig. 9-b). In addition, the baseline curve of spectrum calculated by the $k-\varepsilon$ model, it does not match the experiment beyond 5 kHz.

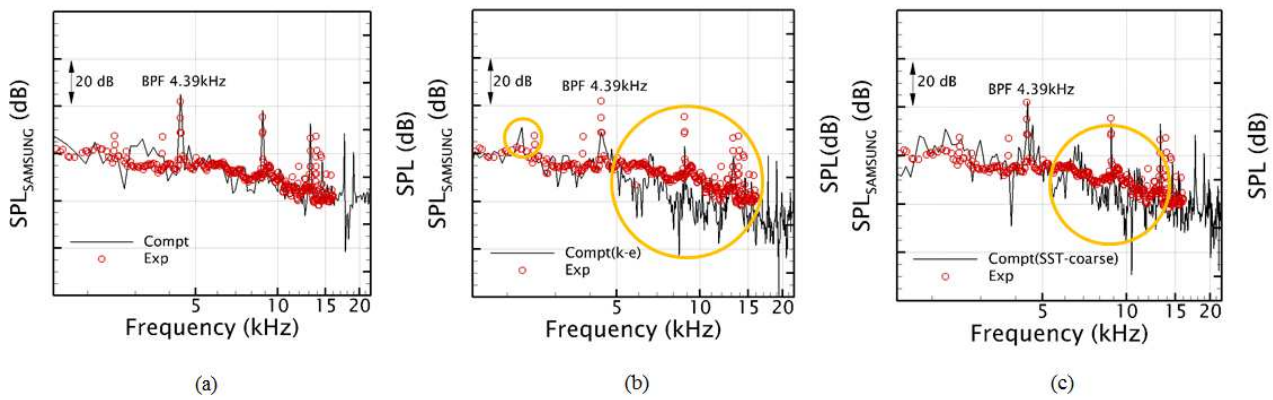


*Figure 9: comparison of numerical near-field pressure fluctuation spectra with the far-field experiment for (7-blade impeller, 16 mm orifice): (a) k-$\omega$ SST turbulence model (11.65 x10$^6$ elements), (b) $k-\varepsilon$ turbulence model (11.65 x10$^6$ elements), (c) k-$\omega$ SST turbulence model with coarse meshes (7.31 x 10$^6$ elements)*

Furthermore, as shown in Figs.9-c, the effect of grid resolution on the spectrum is another important issue for the fan noise characterization. According to these figures, there can be considerable differences in the details of the baseline spectrum obtained by different computational grids. In the case of coarse mesh ($7.31\times10^6$ mesh elements), the baseline of spectrum cannot be preserved beyond 5 kHz due to the mesh resolution (orange circle in Fig.9-c). Even though the result of uRANS is rather sensitive on the numeric, uRANS can provide very promising results with proper turbulence model and well-resolved meshes.

### Consistency of uRANS for impellers with different blade counts

In order to show the consistency of our prediction method, two different impellers at their best efficient point conditions were tested. Two geometrically similar impellers but different blade counts (9 and 13 blades) with the same diffuser, return channel, and AC electric motor were computed. The constant rotational speed, corresponding to the experimental measurement, was imposed to the impeller and the 19 mm orifice diameter was modeled, which is the best efficient point in the aerodynamic performance curve. The near-field pressure fluctuation spectra predicted by uRANS and the far-field sound pressure level of experiments for the 9- and 13-blade impellers are compared in Figs.10-b and c, respectively. As presented, the positions of the BPF and its harmonics and the magnitude of sound pressure level at the BPF are well predicted, and also the spectrum baseline is in good agreement with the experiment.

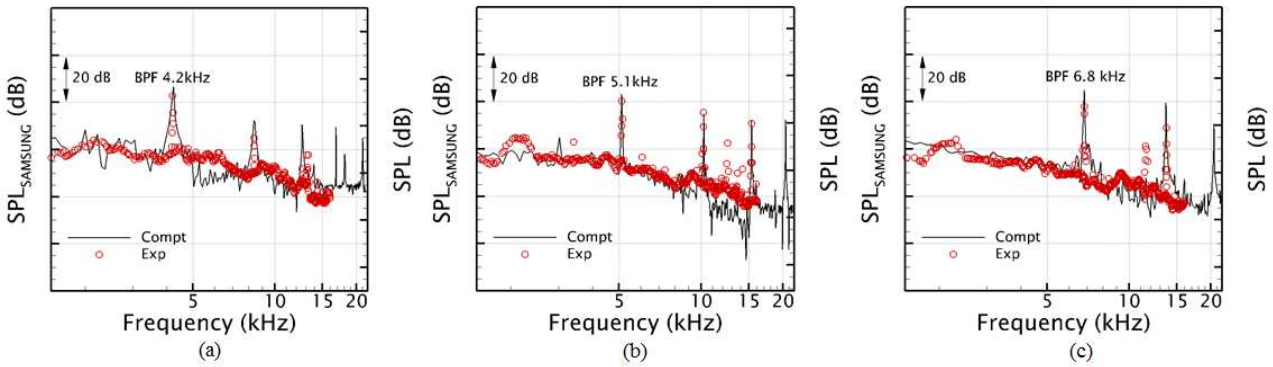


*Figure 10: comparison of numerical near-field pressure fluctuation spectra with far-field experiment for (19 mm orifice): (a) 7 blades, (b) 9 blades, (c) 13 blades*

## NOISE REDUCTION USING SPLITTER

In order to reduce the tonal noise generated by the impeller-diffuser blade interactions, we introduce splitters to reduce the separation region and low momentum flow in the blade passages. As shown in Fig.5, the low momentum flow regions in the blade passages are close to the suction side of the blades due to the leading-edge separation. Splitter, a flow guidance device, is inserted between the blades at the inlet of the flow passages to push the higher momentum flow to the low momentum region and to postpone the separations. Figs.11 depicts the configuration of impeller with and without splitters, respectively.

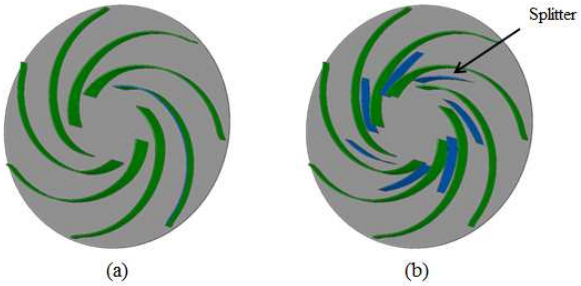


*Figure 11: configuration of impeller (a) without splitter, (b) with splitter*

Two different impeller blade counts (9 and 13 blades) were used to check the effect of splitter in the noise reduction and both cases have the same 19 mm orifice diameter. Figure 12 shows the effect of splitter on the velocity contours at the middle plane of the impeller-diffuser for the 9 and 13 blade impellers. In the case with splitter, the low momentum flow region close to the outlet of the flow passage and separation region at the suction side have been substantially improved and flow field between the blade passages is more uniform compared to the no splitter case.

Fig.13-a compares the near-field pressure fluctuation spectrum calculated by numerical simulations for the 9-blade impeller with and without splitter. By using the splitter, the tonal peak noise at BPF is reduced by 8 dB and also for the following harmonics and the reduction of overall sound pressure level (OASPL) is 6.94 dB. In the case of 13-blade impeller (Fig.13-b), the BPF peak noise and OASPL have been reduced 11 and 4.14 dB, respectively. Effect of splitter on the aerodynamic performance for the centrifugal fans with different blade counts is summarized in table 2. By using the splitter, there is no significant reduction in the vacuum pressure and flow rate in both 9 and 13 blade impellers (less than 1% reduction). Therefore, it is shown that the splitter is a very useful device in terms of noise reduction, especially in tonal noise, without considerable effect on the aerodynamic performance.

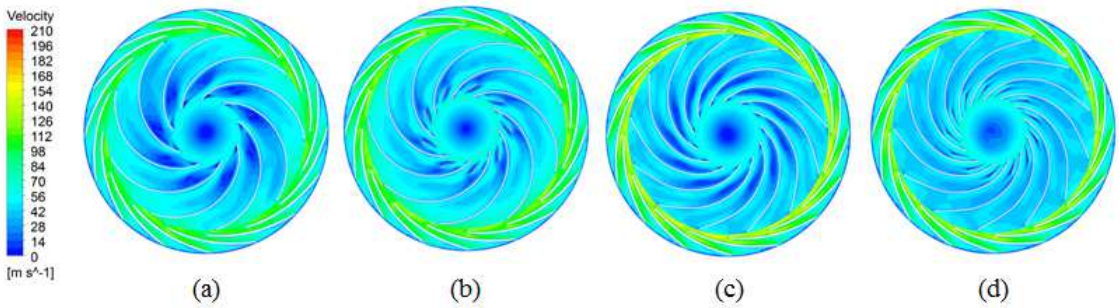


*Figure 12: velocity contour at the impeller-diffuser cross-section plane for impeller (19 mm orifice diameter): 9 blades (a) no splitter, (b) splitter; 13 blades (c) no splitter, (d) splitter*

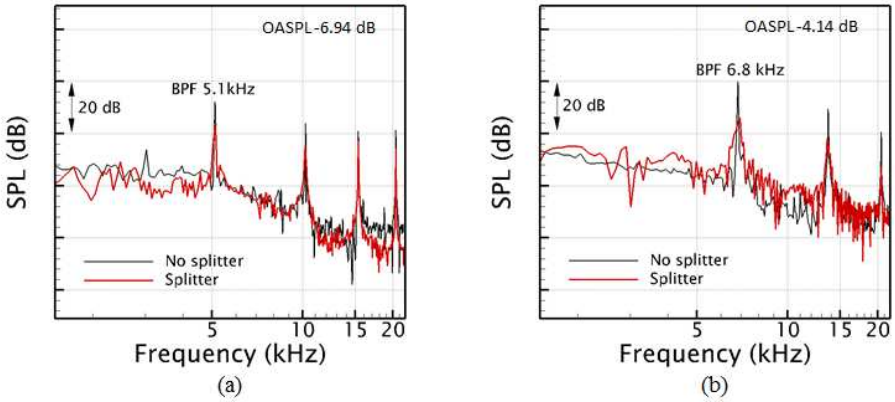


*Figure 13: numerical near-field sound pressure level spectrum with/without splitter for impeller (19 mm orifice diameter): (a) 9 blades, (b) 13 blades*

*Table 2: effect of splitter on the aerodynamic performance for impellers with different blade counts*

| | **9 blades** | | **13 blades** | |
|---|---|---|---|---|
| | **No splitter** | **Splitter** | **No splitter** | **Splitter** |
| **Vacuum pressure (kPa)** | 19.50 | 19.29 | 19.58 | 19.36 |
| **Flow rate (l/sec)** | 25.90 | 25.76 | 25.95 | 25.71 |

# CONCLUSION

A 3D numerical study based on uRANS approach is carried out to simulate the fluid flow in a full scale centrifugal fan, including the impeller, diffuser, return channel and AC electric motor, designed for a vacuum cleaner. Aerodynamic results obtained by numerical computation reveal the details of flow structures in terms of velocity and pressure fields. The agreement between the numerical results is reasonably good in terms of aerodynamic performance analysis, as compared to the experiments.

As far as the fan noise prediction is concerned, it is important to realize that the far-field acoustics are very much dominated by the internal pressure fluctuations originated by the fan inside the fan motor housing. Therefore, the near-field pressure fluctuation spectrum at the impeller–diffuser interface is compared to the far-field sound pressure level spectrum measured by experiments. The results show that with a proper turbulence model and the well-resolved grids for the full-detailed model of the centrifugal fan, the uRANS approach can provide quite promising results compared to the far-field acoustic measurements, not only in prediction of tonal noise but also the broadband noise.

# BIBLIOGRAPHY

[1] W. Neise – *Noise reduction in centrifugal fans: a literature survey*. Journal of Sound and Vibration, 375–403, **1976**

[2] K. R. Fehse, W. Neise – *Generation mechanisms of low-frequency centrifugal fan noise.* AIAA Paper 2370**, 1998**

[3] T. Kudo – *Development of noise-reduction method for radiator fan of automobile*. Japan Society of Mechanical Engineers of Annual meeting lecture collected papers**,** p. 75–6, **2004**

[4] J. S. Choi, D. K. McLaughlin, D. E. Thompson – *Experiments on the unsteady flow field and noise generation in a centrifugal pump impeller.* Journal of Sound and Vibration, 493–514, **2003**

[5] J. Gonzalez, C. Santolaria – *Unsteady flow structure and global variables in a centrifugal pump*. ASME Journal of Fluids Engineering, vol. 128, p. 937-946, **2006**

[6] W. Neise – *Review on noise reduction methods for centrifugal fans.* Journal of Engineering for Industry, 151–161, **1982**

[7] Y. Ohta, E. Outa, K. Tajima – *Evaluation and prediction of blade passing frequency noise generated by a centrifugal blower.* ASME Journal of Turbomachinery, 597–605, **1996**

[8] S. R. Krishna, A. R. Krishna, K. Ramji – *Reduction of motor fan noise using CFD and CAA simulations.* Applied Acoustics Journal, p. 982–992, **2011**

[9] D. Wolfram, T. H. Carolus – *Experimental and numerical investigation of the unsteady flow field and tone generation in an isolated centrifugal fan impeller.* Journal of Sound and Vibration, 4380–4397, **2010**

[10] J. Bardina, P. Huang, T. Coakley – *Turbulence modeling validation.* AIAA Paper 2121, **1997**

[11] Y. G. Bae, J. T. Park, Y. J. Moon – *Internal pressure fluctuations in an air-conditioner indoor unit with cross-flow fan*, in preparation for submission, **2015**